Hudspeth, W.J. (1994) Neuroelectric Eigenstructures of Mental Representation. In D.S. Levine and M. Aparicio IV (Eds.), *Neural Networks for Knowledge Representation and Inference*. Hillsdale, NJ: Lawrence Erlbaum Associates, pp. 419-446. NLP-142

Neuroelectric Eigenstructures of Mental Representation

William J. Hudspeth
Neuropsychometric Laboratory, Radford, Virginia

1. INTRODUCTION

The mechanisms of the human visual system organize neural representations for several levels of knowledge, ranging from simple sensations to complex conceptual processes. A number of methods have been used to investigate the neural processes involved in knowledge representation. These methods range from studies of single neuron activities to imaging techniques (i.e., CAT, PET, & MRI) that reveal activities in large cerebral systems. Since the activities of single neurons and large brain systems can be driven by sensory, perceptual and conceptual conditions of experiments, there is clearly some uncertainty as to how and where the human nervous system represents knowledge. This state-of-the-art suggests that the activities obtained from different levels of neuronal organization may not have the same meaning, and some effort may be required to discover how each level (i.e., neuron-to-system) participates in the knowledge representation process. This discovery process can be subsumed within a single question: How would one recognize and substantiate *knowledge processes* in the varied activities that can be obtained from the human brain?

1.1. BRAIN AND BEHAVIORAL RELATIONSHIPS

The roles of different levels of neuronal organization in knowledge representation are relatively well defined when considered from the perspective of clinical and experimental neuropsychology (Luria, 1973, 1980). This body of knowledge shows that the systems of the brain are organized in hierarchical manner that reflects the psychological attributes of knowledge representation and usage. Fig. 15.1 presents a schematic diagram of this hierarchical organization (Hudspeth, 1985). This diagram shows that the cortical systems for sensory and motor representation are each composed of a primary (Fig. 15.1: I Systems) core which provides an object-oriented computational space for extracting modality specific *images*. Further, each primary system is enclosed within a secondary (Fig. 15.1: II Systems) layer that, by virtue of

learning experiences, images achieve *object constancy* so that objects can be *classified* according to invariant forms and functions (i.e., categories and equivalences). Each of the secondary layers are conjoined by tertiary association structures (Fig. 15.1: III Systems) which assure that sensory specific categories will have equivalent meanings (e.g., reading the word "cat" and hearing the spoken word "cat"). Equally important, the internal core of the limbic system (not shown in Fig. 15.1) provides the organism with basic knowledge of emotions and motives. Thought and behavior are, thus, composed of knowledge of the real world (i.e., from cortical systems I, II & III) and by knowledge of personal emotions/motives (i.e., from the limbic system). The final common strategies for thought and action are coordinated by two well defined compartments of the pre-frontal cortex that have exclusive interconnections with the posterior sensory analyzers (Fig. 15.1: *Fd* System) and the limbic system (Fig. 15.1: *Fo* System), respectively.

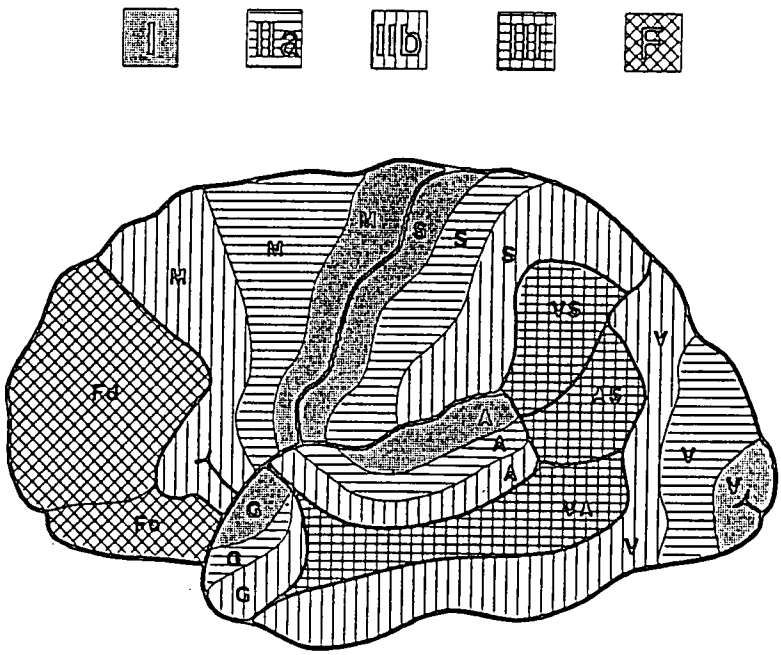

Fig. 15.1. System of cerebral computational compartments which are involved in mental representations. The hierarchical organization is arranged in a top-down manner and designated by the indicated textures for: Frontal (*F*), Tertiary (*III*), Secondary-b (*IIb*), Secondary-a (*IIa*) and Primary (*I*) functions. The primary and secondary functions apply to the sensory and motor processes such as Vision (*V*), Audition (*A*), Gustation (*G*) and the Somatic divisions. The Somatosensory division is partitioned into predominantly Motor (*M*) and Somatosensory (*S*) compartments. Tertiary cross-modal processes are represented by regions within which the principal sensory systems interact: Visuospatial (*VS*), Visuoauditory (*VA*) and Acousticosomatic (*AS*). The frontal executive functions are interconnected to all other systems in a manner that the sensory and motor systems can be regulated by the balance between personal knowledge (*Fd*) and feelings (*Fo*). (From Hudspeth, 1985).

Finally, it is clear that a number of analytic methods could be used to compute structural inter-electrode distances (e.g., coefficients) within a 3-dimensional space. However, in one way another, all of these methods converge on a common source - the outcome is based upon similarities and differences in multichannel SP waveforms which can ultimately be reduced to a small and predictable number of basis waveforms. Therefore, our findings with respect to spontaneous (SP) EEG waveforms provide exceptionally robust support for the primary hypothesis advanced above.

3. KNOWLEDGE REPRESENTATION IN NEUROELECTRIC POTENTIALS

The human ability to formulate concepts provides the basic foundation for most forms of cognitive representation. To achieve higher forms of symbolic representation, an individual must learn to suppress impulsive responses to the concrete aspects of reality, and to mentally transform stimuli, signs or symbols into meaningful equivalents for the real or symbolic world. This ability accrues with age and it changes in qualitative character with each stage of cognitive maturation. For Jean Piaget, such transformations constituted the essential core of human intelligence. Therefore, it is important to ask: How does one go about the task of demonstrating conceptual abilities in particular individuals?

If this question was posed to a clinical psychologist, the answer would be quite straightforward: Simply administer any one of a number of intelligence tests that contain a variety of conceptual problems. However, the results of such testing would not lead an understanding of the knowledge representation process. On the other hand, if this question was posed to a mathematical psychologist, the answer could be formulated in a structural manner that allows different perceptual and conceptual (i.e., stimulus) attributes to be related to each other by means of similarities and differences in their meanings. Such formulations are equations by which the elements of knowledge can be represented in classes, categories, and hierarchies. Therefore, the neurophysiological studies in my laboratory have been directed toward this second form of conceptual representation.

Studies of the evoked, or event-related, potential (EP) have been related to all levels of brain function, and several reviews provide substantial evidence for the richness of this method (Regan, 1972; Hillyard, Picton & Regan, 1978; Hillyard & Picton, 1979; John & Schwartz, 1978; Boddy, 1985). These reviews show that there are two general perspectives in the use and interpretation of the EP. These perspectives can be differentiated according to the basic indices extracted from the EP for analysis and inference.

While the EP is a complex waveform of 0.5 to 1.0 sec duration, a number of workers have found that single voltage peaks, confined to specific time-latencies (i.e., the P300), are strongly influenced by general states related to cognitive functions, such as attention, selective attention and certainty-uncertainty. It is important to identify the unit of measurement used in such studies, because the conclusions that can be drawn from these investigations are limited. For example, if a human observer's selective attention covaries with the relative amplitude of the P300 component of the EP waveform, inferences concerning selective attention can only vary along a unidimensional vector. Therefore, it can be seen that single peak components of the EP do not provide inferences concerning classes, categories, or hierarchies that are inherently multidimensional in their structure.

1.2. STRUCTURE OF KNOWLEDGE PROCESSES

Knowledge processes represent an organism's attempt to *interpret* the identity of objects and events that occur in the internal and external world. The ability to extract reliable and invariant interpretations of the dynamic environment is essential for the survival and successful adaptation of the individual organism. This ability depends upon both genetic and experiential factors that begin with conception and are then continually refined over decades of life.

One source of evidence for the structure of knowledge can be found, for example, in the stages of cognitive maturation as described by Jean Piaget (1963), and subsequently extended by several other workers (Case, 1992; Stuss, 1992; Vandermaas & Molenaar, 1992; and van Geert 1991). Several recent studies of brain electrical activities show that the maturation of the regional brain systems, as shown in Fig. 15.1, coincide with the stages of cognitive maturation originally set forth in Piaget's work, and in the aforementioned Neo-Piagetian studies (Hudspeth, 1985, 1987; Hudspeth & Pribram, 1990, 1992; Thatcher, Walker & Guidice, 1987, and Thatcher, 1991). Therefore, it can seen that the study of electrical activities arising from the brain's computational compartments can provide substantial information about the neurobiological organization of knowledge representation in the human brain.

A second source of evidence for the structure of knowledge may be found in detailed investigations of the nature of *mental* representation within the brain's computational systems. In mathematical psychology, for example, mental representations are defined by the quantitative relationships among different categories of experience (Shepard & Chipman, 1970; Shepard, 1975, 1978; Shepard, Kilpatric & Cunningham, 1975). This approach assumes that human experience and knowledge is multidimensional in nature and can be represented by vector subspaces within an n-dimensional geometry. This notion is consistent with a traditional structural definition of human knowledge which is based upon a taxonomy of exemplars, classes, categories, and hierarchies.

1.3. BRAIN ELECTRICAL ACTIVITIES

The human electroencephalogram (EEG) is a record of spontaneous potential (SPs) oscillations that can be readily obtained from a resting subject using scalp electrodes. When external stimuli are presented to attentive subjects, time-locked evoked potentials (EPs) appear in the SP, such that the obtained recordings contain both SP and EP waveshape components.

From 1985 to 1988, my students (Joel Alexander and Chris Ludwig) and I carried out detailed investigations on the structural analysis of the human electroencephalogram, using both SP and EP waveforms. Although the methods we used have been applied by other workers, the approach and design of our experiments were sufficiently unique that it seems likely that we may have discovered a basic principle by which the EEG represents the computational *compartments* of the brain (as in Fig. 15.1) and, as well, the computational *operations* by which those compartments make knowledge representation possible. It will be shown that this basic principle provides nearly perfect *a priori* predictions for the outcome of EEG investigations using either SP or EP waveforms. This primary principle can be stated in the following manner:

Hypothesis: The EEG (SP or EP) waveform is a linear combination of N orthogonal basis waveforms (eigenvectors) which are sufficient in number to span an N-dimensional attribute space composed of K forcing agents (exemplars).

2. FUNCTIONAL ARCHITECTURE OF NEUROELECTRIC POTENTIALS

Neuroanatomists describe the brain's functional compartments and fiber connections by means of exquisitely stained histological sections that reveal an integrated system which is designed to achieve the smooth coordination of functionally distinct activities. By tradition, these neurohistological details are represented on 3 anatomical planes (horizontal (top); sagittal (side) and coronal (front)), so that each perspective can index the relative position of each functional compartment and their interconnections within a 3-dimensional space. It is important to note that highly related functional compartments are connected by means of short-distance horizontal fibers, and conversely, that relatively unrelated functional compartments are integrated by means of long-distance fiber connections. Therefore, it seems likely that the SP waveforms obtained from multichannel EEG recordings from the entire cerebral surface would reflect both the uniqueness of different functional compartments, and as well, their integration by means of short and long distance connections.

To test this proposition, we implemented the primary hypothesis, noted above, in the following way: A.) We defined the number of attribute dimensions as $N=3$, so as to span the cortical surface in a way that would encompass the horizontal, sagittal and coronal boundaries within which all of the computational compartments are confined; and B.) We defined the number of forcing agents as $K=19$, equal to the number of functional compartments, as represented by samples of SP waveforms obtained from 19 recording electrodes (exemplars) on the scalp surface.

We obtained multichannel ($K = 19$) SP waveforms (1 minute recordings) from 25 subjects, with two replications from each subject. We then computed all combinations of similarities and differences (using correlation coefficients) among the $K = 19$ SP waveform recordings to produce a triangular correlation matrix for each subject and replication. The correlation matrices were factored with principal components analysis to obtain 3 eigenvectors (basis waveshapes) and the weighting coefficients required to project each of the $K = 19$ electrodes into a 3-dimensional geometric representation of the cortical surface. On the average, these analyses accounted for 85% of the covariation among the 19 SP waveforms obtained from each subject and replication.

Fig. 15.2 shows the averaged coefficients for 50 SP recordings. As can be seen, the 19 electrodes are positioned in 3-dimensional space at the approximate locations recording electrodes are positioned on the scalp. The contour mappings on the bottom, side and rear panels (e.g., horizontal, sagittal and coronal planes, respectively) reveal functional nonlinearities (i.e., inequalities in electrode distances) that can reliably be manipulated by opening and closing the subject's eyes (Hudspeth, Alexander & Garrett, 1993; Hudspeth, 1993a). These findings show that multichannel SP waveforms can be encompassed by 3 basis waveforms that account for the overall integration of the functional compartments of the cerebral cortex. The findings also reveal that individual electrodes are positioned within this integrated system according to the similarities and differences among the multichannel SP waveforms, in such a way as to index

their membership with specific cortical functions. Despite subtle individual differences in SP waveforms, the results obtained with these structural coefficients are virtually predictable across subjects, except in cases of neuropathology.

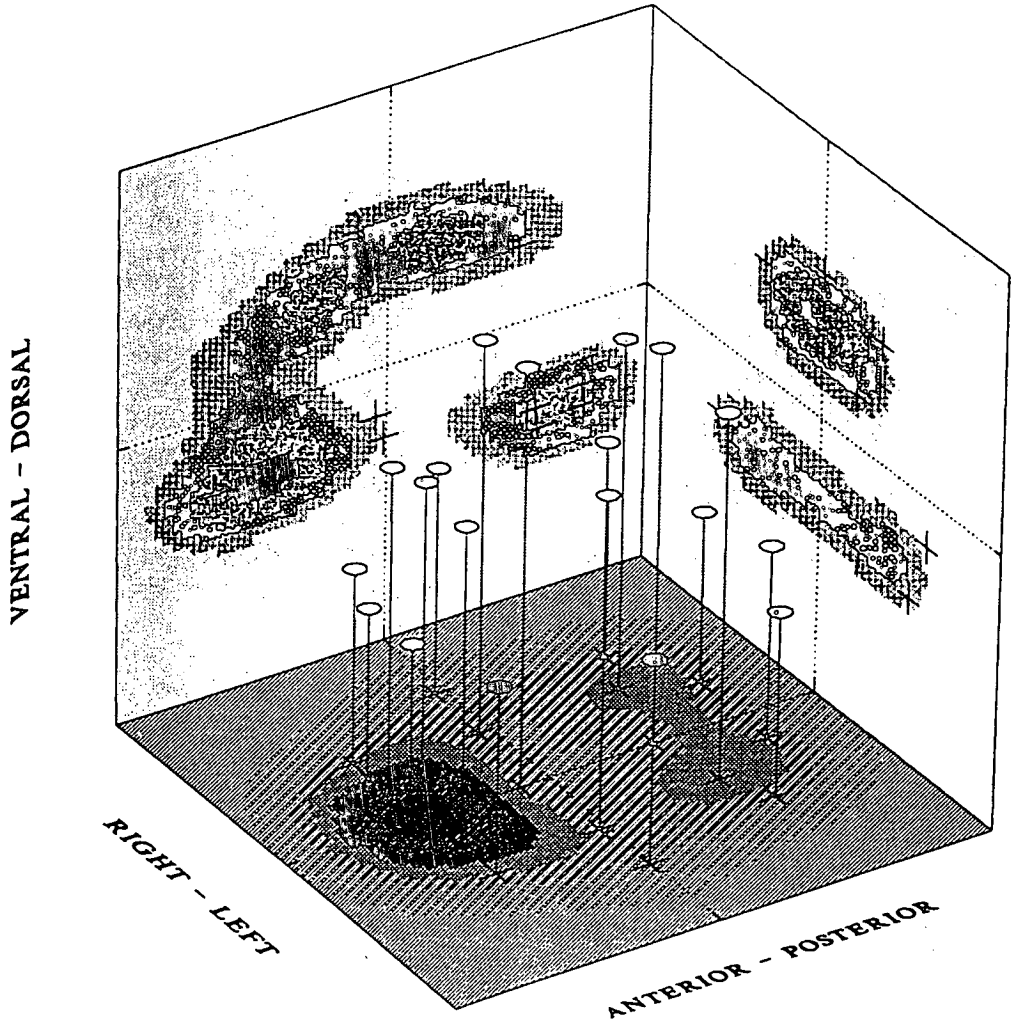

Fig. 15.2. Present a 3-dimensional mapping of the functional architecture of the spontaneous EEG. The distribution of recording electrodes is based upon three basis waveforms extracted from a 19-channel recording of spontaneous EEG activity by means of principal components analysis. The exact position of each electrode is determined by the weighting coefficients for the three PCA components. The gradient mappings on the base, side and rear walls index the density of electrode clustering on the horizontal, sagittal and coronal planes. Individual electrode positions are indicated by plus (+) signs. (From: Hudspeth, 1993a; Hudspeth, Alexander & Garrett, 1993).

Finally, it is clear that a number of analytic methods could be used to compute structural inter-electrode distances (e.g., coefficients) within a 3-dimensional space. However, in one way another, all of these methods converge on a common source - the outcome is based upon similarities and differences in multichannel SP waveforms which can ultimately be reduced to a small and predictable number of basis waveforms. Therefore, our findings with respect to spontaneous (SP) EEG waveforms provide exceptionally robust support for the primary hypothesis advanced above.

3. KNOWLEDGE REPRESENTATION IN NEUROELECTRIC POTENTIALS

The human ability to formulate concepts provides the basic foundation for most forms of cognitive representation. To achieve higher forms of symbolic representation, an individual must learn to suppress impulsive responses to the concrete aspects of reality, and to mentally transform stimuli, signs or symbols into meaningful equivalents for the real or symbolic world. This ability accrues with age and it changes in qualitative character with each stage of cognitive maturation. For Jean Piaget, such transformations constituted the essential core of human intelligence. Therefore, it is important to ask: How does one go about the task of demonstrating conceptual abilities in particular individuals?

If this question was posed to a clinical psychologist, the answer would be quite straightforward: Simply administer any one of a number of intelligence tests that contain a variety of conceptual problems. However, the results of such testing would not lead an understanding of the knowledge representation process. On the other hand, if this question was posed to a mathematical psychologist, the answer could be formulated in a structural manner that allows different perceptual and conceptual (i.e., stimulus) attributes to be related to each other by means of similarities and differences in their meanings. Such formulations are equations by which the elements of knowledge can be represented in classes, categories, and hierarchies. Therefore, the neurophysiological studies in my laboratory have been directed toward this second form of conceptual representation.

Studies of the evoked, or event-related, potential (EP) have been related to all levels of brain function, and several reviews provide substantial evidence for the richness of this method (Regan, 1972; Hillyard, Picton & Regan, 1978; Hillyard & Picton, 1979; John & Schwartz, 1978; Boddy, 1985). These reviews show that there are two general perspectives in the use and interpretation of the EP. These perspectives can be differentiated according to the basic indices extracted from the EP for analysis and inference.

While the EP is a complex waveform of 0.5 to 1.0 sec duration, a number of workers have found that single voltage peaks, confined to specific time-latencies (i.e., the P300), are strongly influenced by general states related to cognitive functions, such as attention, selective attention and certainty-uncertainty. It is important to identify the unit of measurement used in such studies, because the conclusions that can be drawn from these investigations are limited. For example, if a human observer's selective attention covaries with the relative amplitude of the P300 component of the EP waveform, inferences concerning selective attention can only vary along a unidimensional vector. Therefore, it can be seen that single peak components of the EP do not provide inferences concerning classes, categories, or hierarchies that are inherently multidimensional in their structure.

The second perspective is composed of EP studies which are based upon the analysis of complete EP waveforms that can provide a dimensionality of $N > 1$. Of particular interest here, are those studies which show that EPs have similar waveforms when the evoking stimuli have similar interpretations, and conversely, that EPs have dissimilar waveforms when the evoking stimuli have dissimilar interpretations (John, Harrington & Sutton, 1967; John, 1977; Johnston & Chesney, 1974; Begleiter & Porjesz, 1975; Begleiter, Porjesz & Garozzo, 1979; Shelburne, 1978; Buchsbaum, Coppola & Bittker, 1974; Teyler, Roemer, Harrison & Thompson, 1973; Roemer & Teyler, 1977). Such findings imply that mental representations, as reflected in neuroelectric signals, could be accomplished by means of neuroanatomical computations that entail eigenfunctions, as proposed in the primary hypothesis above.

3.1. MODELS OF MENTAL REPRESENTATION

Throughout this chapter, I have carefully applied the terms *similar* (-ities) and *dissimilar* (-ities) because they provide the means with which to develop formal *a priori* predictions concerning the cerebral generation of both SP and EP waveforms. Just as mathematical psychologists use *conjoint* similarities and dissimilarities to describe the structures of mental representation at the behavioral level, it seems likely also that the neurobiological processes of mental representation could be revealed by means of the same strategies. The studies presented below show that the *a priori* prediction of EP waveforms depends upon the application of *conjoint* similarities-differences, both in the selection of stimulus attributes and in the analysis of the resulting EP waveforms.

We implemented this strategy by selecting stimulus attributes in such a way as to construct what we call an *orthogonal stimulus set*, which was then followed by an appropriate analysis that was designed to recover the orthogonalized stimulus attributes within the resulting EP waveforms for each stimulus set, as a whole. In the two examples presented below, each stimulus set contained four stimuli, and each of the four stimuli was composed of two independent attribute dimensions. Figs. 3 and 4 present these examples as a matrix of stimulus attributes (Figs. 15.3A & 15.4A) and in the form of an *a priori* predictor model (Figs. 3B & 4B).

Fig. 15.3A presents a stimulus matrix for a form-color classification (Hudspeth, 1993). As may be seen, the form dimension is composed of two exemplars — circles and triangles. Similarly, the color dimension is composed of two exemplars — red and green. It follows, therefore, that each stimulus is composed as 50%-form and 50%-color. As with any 2x2 matrix of fully nested attributes, the column means (i.e., C1 & C2) are expected to reflect the unitary influence of the color attributes, green and red, respectively. Similarly, the row means (i.e., F1 & F2) are expected to reflect the unitary influence of the form attributes, circle and triangle, respectively. Finally, the grand mean (i.e., CF) is expected to reflect the only common attribute which is shared among the four stimuli, which, by definition, should not contain form or color information. The stimulus matrix can be translated into an *a priori* prediction model by considering the proportion of variance each attribute contributes to each of the cells in the stimulus matrix. As can be seen in Fig. 15.3B, the distribution of attributes among the cells of the stimulus matrix can be represented by the sines and cosines of a unit-circle, and by noting that the squared sines and cosines are proportions. Since the grand mean (i.e., CF) of the

stimulus matrix contains none of the form-color attributes, it represents the origin of the unit-circle, set at x = 0, y = 0.

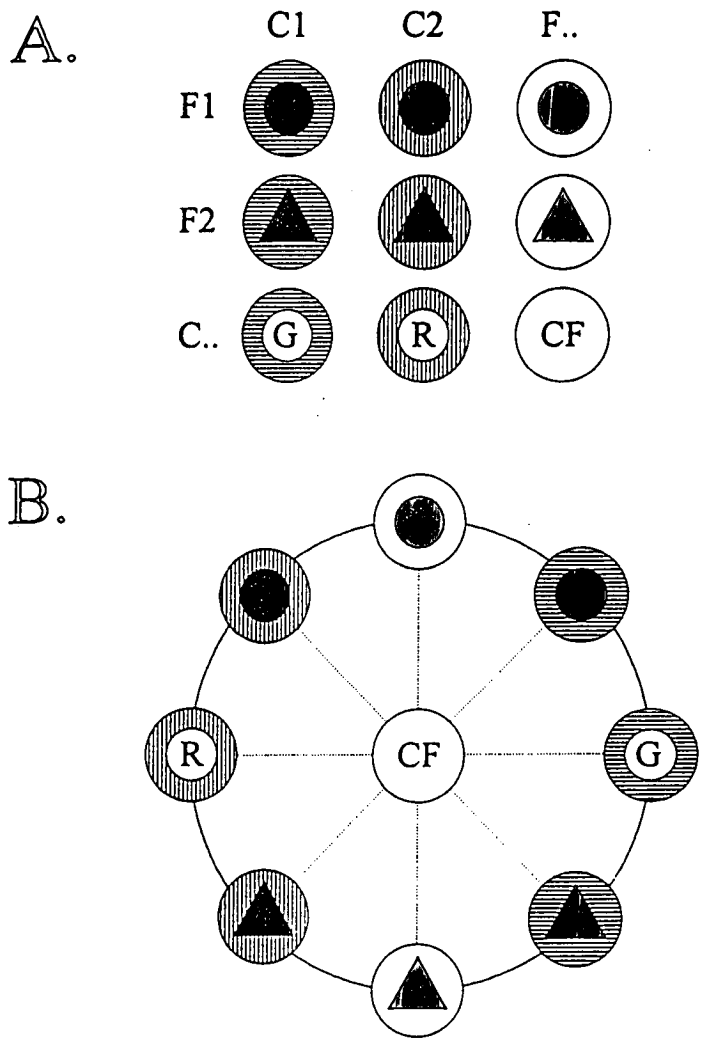

Fig. 15.3. Fig. 15.3A presents the orthogonal stimulus matrix used in the form-color classification experiment. Form attributes are identified with the appropriate form shapes. Color attributes are identified with background hatching, where green colors have horizontal background lines and red colors have vertical background lines. The column and row means are indexed according to the same form and color graphing keys. Fig. 15.3B shows the *a priori* predictor model by which the form and color features of the stimulus set were positioned on the circumference of a unit-circle. A sine-cosine list specifies the position of each stimulus on the X (color) and Y (form) dimensions. The squared sines and cosines can also be used to estimate the proportion of variance each attribute contributes to the stimuli in the set (From: Hudspeth, 1993a, 1993b).

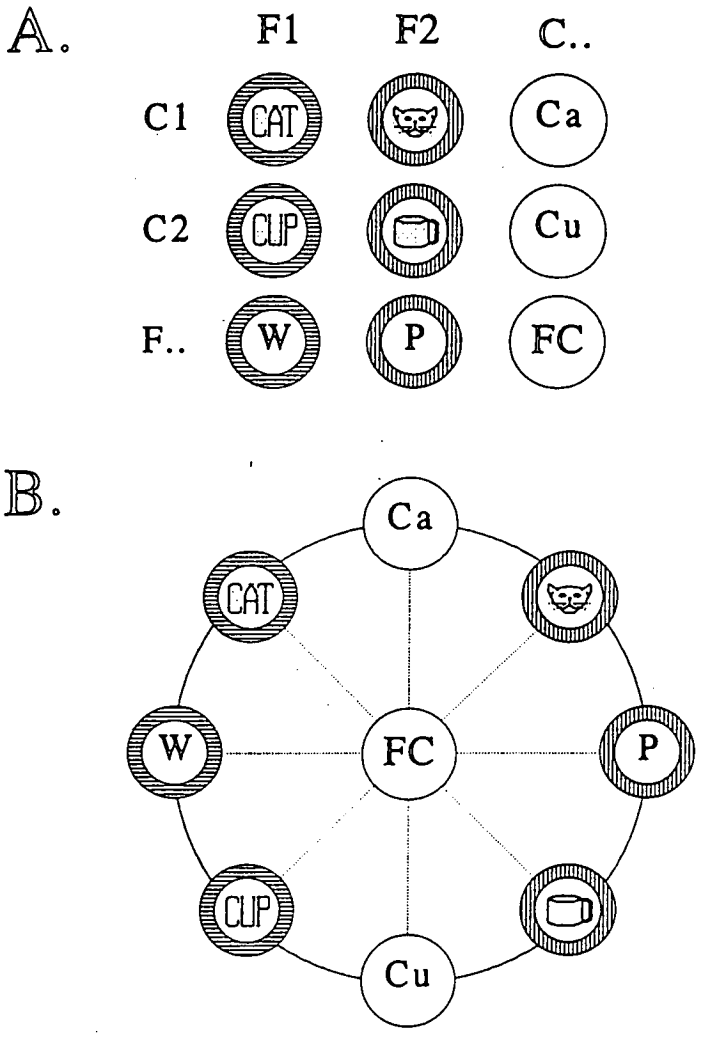

Fig. 15.4. Fig. 15.4A presents the orthogonal stimulus matrix used in the concept-format classification experiment. Concept attributes are identified by the cat and cup stimuli used. Format attributes are identified by the actual word and picture stimuli used. All word stimuli (W) have a horizontal line background and all picture (P) stimuli have a vertical line background. The concepts of cat (Ca) and cup (Cu) are identified by the letter symbols Ca and Cu, respectively. Fig. 15.4B shows the *a priori* predictor model by which the concept and format features of the stimulus set were positioned on the circumference of a unit-circle. In this case the stimuli are numbered: 1 - cat mean, 2 - picture cat, 3 - picture mean, 4 - picture cup, 5 - cup mean, 6 - word cup, 7 - word mean and 8 - word cat. A sine-cosine list specifies the position of each stimulus on the X (format) and Y (concept) dimensions. The squared sines and cosines can also be used to estimate the proportion of variance each attribute contributes to the stimuli in the set (From: Hudspeth, 1993a; Hudspeth & Alexander, 1993).

Fig. 15.4A presents a stimulus matrix for an object concept-symbol format classification (Hudspeth & Alexander, 1993). As may be seen, the object concept dimension is composed of two exemplars — cat and cup. Similarly, the symbol format dimension is composed of two exemplars — word and picture. It follows, therefore, that each stimulus is composed as 50%-object concept and 50%-symbol format. As with any 2x2 matrix of fully nested attributes, the column means (i.e., F1 & F2) are expected to reflect the unitary influence of the format attributes, word and picture, respectively. Similarly, the row means (i.e., C1 & C2) are expected to reflect the unitary influence of the concept attributes, cat and cup, respectively. Finally, the grand mean (i.e., FC) is expected to reflect the only common attribute which is shared among the four stimuli, which, by definition, should not contain format or concept information. This stimulus matrix can be translated into an *a priori* prediction model by means of the same transformations described in the case of the form-color classification above (e.g., Fig. 15.3B).

3.2. ANALYTIC COMPUTATION OF EP BASIS WAVEFORMS

We obtained visual EP waveforms from normal subjects while they were comfortably seated in a quiet darkened room. EP waveform recordings were synchronized with stimulus presentations on a computer CRT monitor so that the EP waveforms would contain information about the evoking stimuli. Two different groups of subjects served in the form-color and concept-format studies (i.e., Figs. 3 & 4), respectively, and the details of our procedure can be found in other works (Hudspeth, 1993). The EP waveforms for each stimulus set were carefully edited by visual inspection to delete data with muscle or movement artifacts from further analysis. Our analyses were focused upon the changes in EP waveforms at each recording location on the scalp so that we could describe the characteristic computations within each cortical compartment. To achieve this end, we constructed data files that contained eight (8) EP waveforms so as to represent each cell of the stimulus matrix (i.e., Figs. 3A & 4A) and position on the unit-circle predictor model (i.e., Figs. 15.3B & 15.4B).

Principal components analysis (PCA) was used to compute and weight N orthogonal basis waveforms for each EP data file. This method allowed us to determine the exact composition of each of the 8 EP waveforms (i.e., representing the stimulus matrix) as a linear combination of the resulting basis waveforms (eigenvectors). The results of PCA analyses for the two experiments provide robust support for the primary hypothesis presented earlier.

Fig. 15.5 presents PCA results from the form-color classification experiment (i.e., green circle, green triangle, red circle, red triangle), consisting of the averaged EP waveforms obtained from the right parietal electrode in eight normal subjects (Hudspeth, 1993). The first column of Fig. 15.5A shows the averaged EP waveforms obtained for each position of the unit-circle (e.g., Clockwise from 0°: CM, GC, GM, GT, TM, RT, RM, RC). These EP waveforms can be decomposed into a linear combination of three basis waveforms (i.e., components 1, 2 & 3). The first basis waveform (Column 2, Component 1), accounts for a common feature in all 8 EP waveforms, which is due to a common forcing agent — the photic energy used to present the stimulus information on a CRT screen. For this reason, Component 1 is frequently called the *exogenous* EP waveform component. It can be seen that Component 1 does not provide information about attributes embedded in the stimulus set (i.e., form or color). The second basis waveshape (Component 2, Column 3) accounts for the *form* forcing agent, such that circle

exemplars are composed of basis waveforms having negative weighting coefficients, and triangle exemplars are composed of basis waveforms having positive weighting coefficients. The third basis waveform (Component 3, Column 4) accounts for the *color* forcing agent, such that green exemplars are composed of basis waveforms having negative weighting coefficients, and red exemplars are composed of basis waveforms having positive weighting coefficients. Finally, Column 5 shows that the Residual waveforms contain little if any information (i.e., no more than 0.8%).

Fig. 15.5B sets the stage for a discussion of the cortical computations that are entailed in knowledge or mental representation by summarizing the PCA findings with specific reference to the column and row means of the stimulus matrix (Fig.3A). It will be recalled that we expected the column means (Fig. 15.3A: C1 & C2) would contain only color information, and the row means (Fig. 15.3A: F1 & F2) would contain only form information. Fig 5A verifies these expectations. As can be seen in Fig. 15.5B, circle and triangle EP waveforms vary symmetrically around the exogenous EP waveform component (Column 1), and similarly, green and red EP waveforms vary symmetrically around the exogenous EP waveform (Column 2). Thus, the basis waveforms for form information (Column 3) are simply mirror-images of a single dimensioned waveform vector, and similarly, the basis waveforms for color information (Column 4) are simply mirror-images of an orthogonal waveform vector. All of these findings satisfy the requirements for constructing a *conceptual transfer function,* based upon a unit-circle representation of the EP waveform results obtained from specific stimulus sets.

Fig. 15.7 presents PCA results from the concept-format classification experiment (i.e., word "cat", word "cup", picture cat, picture cup), consisting of the averaged EP waveforms obtained from the right dorso-frontal electrode in a normal subject (Hudspeth & Alexander, 1993). It should be noted here that, when using complex visual stimuli, individual differences in EP waveforms were sufficiently large that signal averaging should not be used. However, once the basis waveshapes and weighting coefficients have been computed, group averages can be obtained as before. The first column of Fig. 15.7A shows the averaged EP waveforms obtained for each position of the unit-circle (e.g., Clockwise from 0°: AM, PA, PM, PU, UM, WU, WM, WA). These EP waveforms can be decomposed into a linear combination of three basis waveforms (i.e., components 1, 2 & 3). The first basis waveform (Column 2, Component 1), accounts for a common feature in all 8 EP waveforms, which is due to the *exogenous* EP waveform component. As before, Component 1 does not provide information about attributes embedded in the stimulus set (i.e., concept or format). The second basis waveshape (Component 2, Column 3) accounts for the *concept* forcing agent, such that cat exemplars are composed of basis waveforms having negative weighting coefficients, and cup exemplars are composed of basis waveforms having positive weighting coefficients. The third basis waveform (Component 3, Column 4) accounts for the *format* forcing agent, such that picture exemplars are composed of basis waveforms having negative weighting coefficients, and word exemplars are composed of basis waveforms having positive weighting coefficients. Finally, Column 5 shows that the Residual waveforms contain a small and insignificant amount of systematic information (i.e., no more than 6.3%).

Fig. 15.7B sets the stage for a discussion of the cortical computations that are entailed in knowledge or mental representation by summarizing the PCA findings with specific reference to the column and row means of the stimulus matrix (Fig.4A). It will be recalled that we expected

the column means (Fig. 15.4A: F1 & F2) would contain only format information, and that the row means (Fig. 15.3A: F1 & F2) would contain only concept information. Fig 6A verifies these expectations. As can be seen in Fig. 15.7B, cat and cup EP waveforms vary symmetrically around the exogenous EP waveform component (Column 1), and similarly, picture and word EP waveforms vary symmetrically around the exogenous EP waveform (Column 2). Thus, the basis waveforms for concept information (Column 3) are simply mirror-images of a single dimensioned waveform vector, and similarly, the basis waveforms for format information (Column 4) are simply mirror-images of an orthogonal waveform vector. All of these findings satisfy the requirements for constructing a *conceptual transfer function,* based upon a unit-circle representation of the EP waveform results obtained from specific stimulus sets.

3.3. CORTICAL COMPUTATION OF BASIS WAVEFORMS

In an effort to avoid any form of analytic solipsism, we have analyzed our data sets with many different methods. Our preferred analysis, PCA, is only one among a number of analytic methods that could be used to decompose an 8-EP waveform data set into its constituent basis waveforms. However, it will be shown here that the brain appears to use very elegant processes to orthogonalize stimulus attributes in a way that accomplishes conceptual classifications, and that these outcomes (i.e., transfer functions) can be demonstrated with no more analytic power than *addition, subtraction and division.* The key to this analytic power arises from the design of the orthogonal stimulus set and the expected allocation of attribute variances within a stimulus matrix (e.g., Figs. 3A & 4A).

The expected allocation of attribute variance are stated above with respect to the composition of EP waveform averages for the columns and rows of the stimulus matrix. According to the analytic results from PCA, each column of the stimulus matrix is represented by a single EP basis waveform which is simply sign-reversed to reflect the two exemplars on the column dimension. Similarly, each row of the stimulus matrix is represented by an orthogonal basis waveform, which is sign-reversed to reflect the two exemplars on the row dimension. Therefore, it follows that if the EP waveforms for the column and row attributes are averaged (i.e., addition, division) into their respective marginal cells, and the grand mean (e.g., exogenous EP waveform) of the stimulus matrix is removed (i.e., addition, division, subtraction) from the remaining EP waveforms, then the column and row marginal deviation EP (ΔEP) waveforms should reproduce the basis waveforms obtained from the considerably more complex PCA procedure.

Fig. 15.5. Fig. 15.5A presents the results of a principal components analysis (PCA) for the right parietal (P4) electrode in the form-color classification experiment. Column 1 presents the ORIGINAL EP waveforms for the 8 stimulus positions on the unit-circle model: CM - circle mean, GC - green circle, GM - green mean, GT - green triangle, TM - triangle mean, RT - red triangle, RM - red mean and RC - red circle. Column 2 presents Component 1, the exogenous basis waveform for each stimulus position. Column 3 presents Component 2, the form basis waveform for each stimulus position. Column 4 presents Component 3, the color basis waveform, for each stimulus position. Column 5 presents the RESIDUAL waveform which obtains after removal of the first three basis waveforms. Weighting coefficient are presented to the left of each basis and residual waveform

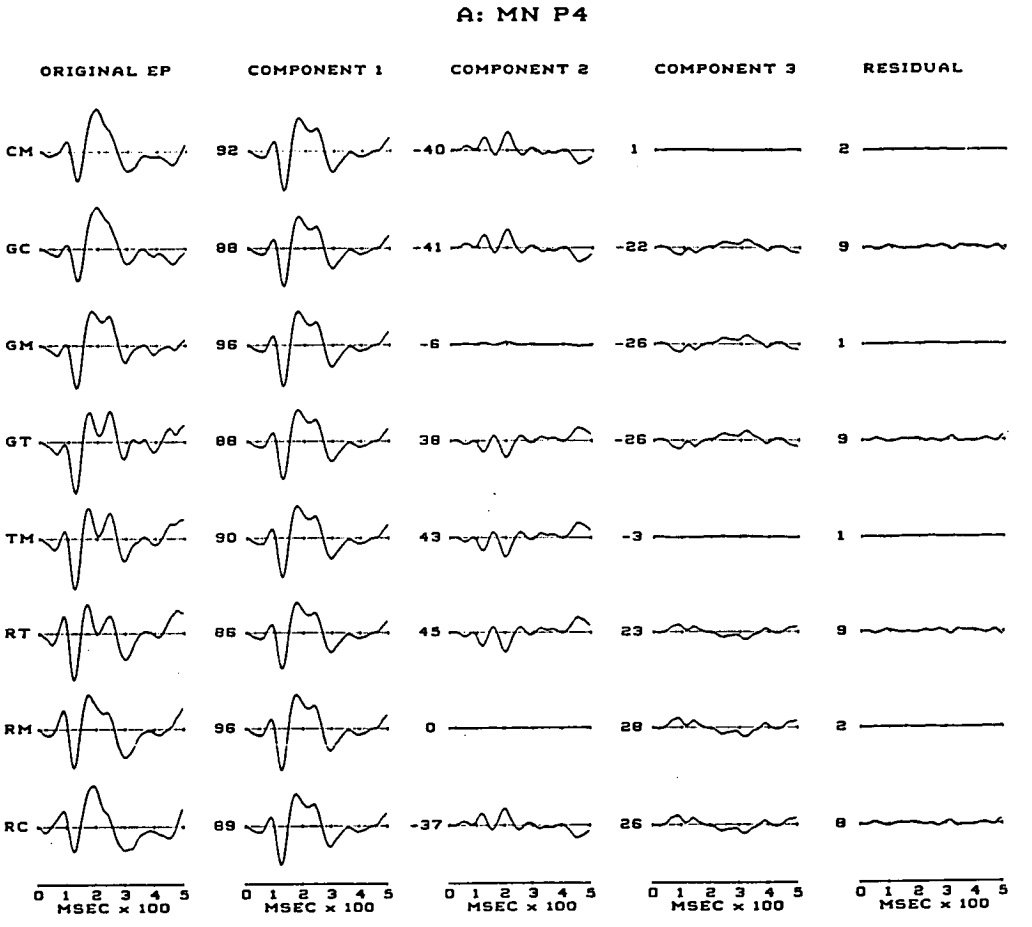

to index the magnitude of the specific basis waveform. The coefficients should be read as C/100 as they were scaled for printing. A 500 millisecond time index is placed under each of the five waveform columns. Fig. 15.5B present a SUMMARY of the PCA findings for the P4 electrode that is formatted for direct comparisons with the calculations shown in Fig. 15.6. The text describes these comparisons. (From Hudspeth, 1993a).

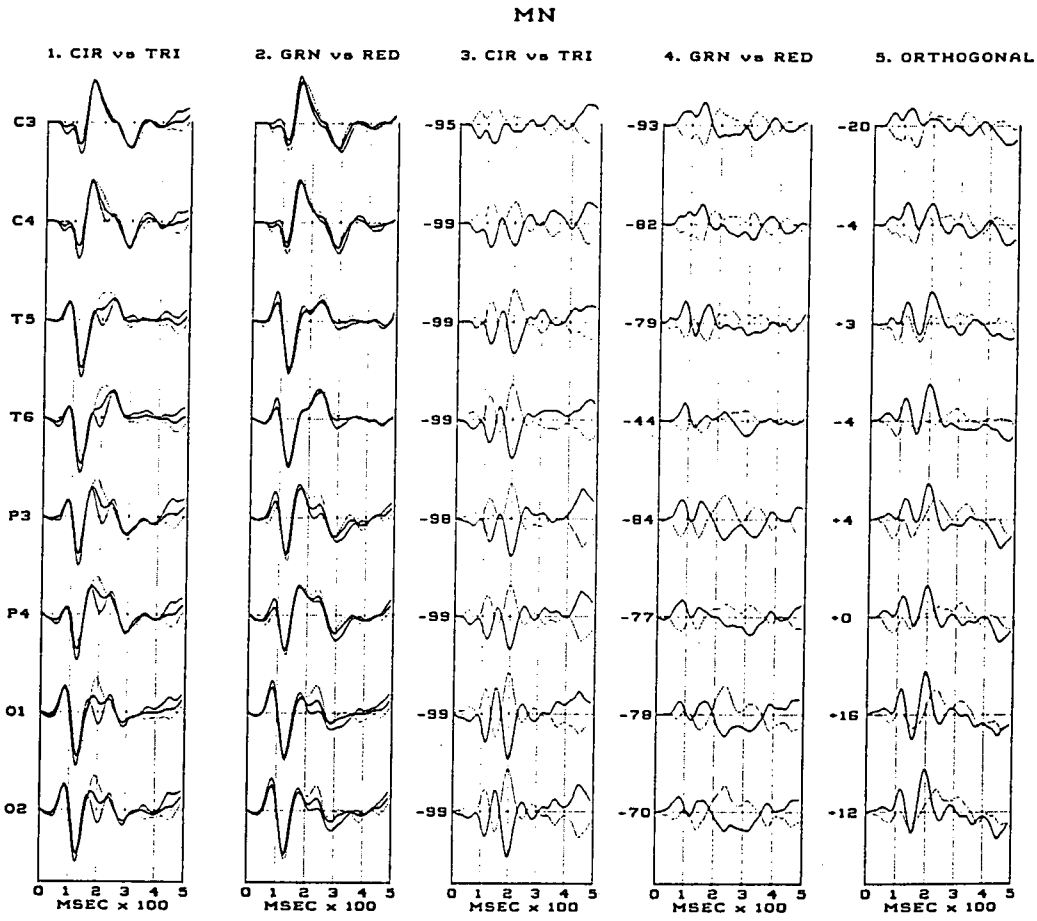

Fig. 15.6. Presents the EP and ΔEP waveforms obtained for the form-color classification experiment. Columns 1 presents the EP waveforms for the circle and triangle means. Note that, at each electrode location, these waveforms deviate symmetrically around the local exogenous EP waveform (shown as a thick line). Similarly, Columns 2 presents the EP waveforms for the green and red means. Note that, at each electrode location, these waveforms also deviate symmetrically around the local exogenous EP waveform (shown as a thick line). When the local exogenous EP waveform was removed, ΔEP waveform-pairs for the form axis and the color axis were nearly identical and sign-inverted. In contrast, ΔEP waveform-pairs for the orthogonal axes were effectively uncorrelated. The sign and magnitude of the squared correlation coefficients (r^2) for each pair of ΔEP waveform is presented to the left of the tracings for each recording location and axis comparison (form, color and orthogonal). *Data Tracings:* Each waveform-pair is composed of dotted and solid line tracings that identify primary features named in each Figure heading. In all cases, the first named feature is the dotted line, and the second named feature is the solid line. *Scaling Factors*: The epoch length of each waveshape was 500 msec, using 100 points with 5 msec/point resolution. The amplitude of all EP waveforms was equated by transformation to a Z-Score scale with a Mean = 0, and σ = 1.0. Please note that the scaling for ΔEP waveforms is twice that of EP waveforms.

We tested this hypothesis with data sets obtained from the form-color classification experiments (Hudspeth, 1993). Fig. 15.6 presents the results of these calculations for the 8 electrode locations from which we obtained data. These findings are presented in the same format as those shown in the Summary of PCA results presented in Fig. 15.5B. For a direct comparison, note the electrode identified as 'P4' in Fig. 15.6. It can be seen that the EP waveforms for circle and triangle in Fig. 15.6 (Column 1) vary symmetrically around the exogenous EP waveshape computed for the CF cell of the stimulus matrix. Similarly, the EP waveforms for green and red in Fig. 15.6 (Column 2) also vary symmetrically around the exogenous EP waveshape. While the EP waveforms for each stimulus are obviously the same as those depicted in Fig. 15.6B, note that the exogenous EP waveform in Fig. 15.6: (CF average) is identical to the exogenous basis waveform (Component 1) obtained from the PCA method. Similarly, the ΔEP waveform-pairs for circle and triangle in Fig. 15.6 (Column 3) are identical in shape and polarity to the second basis waveform (Component 2) obtained from the PCA method (Fig. 15.5B). Finally, the ΔEP waveform-pairs for green and red in Fig. 15.8 (Column 4) are nearly identical in shape and polarity to the third basis waveform (Component 3) obtained from the PCA method (Fig. 15.5B).

Fig. 15.6 shows that the ΔEP waveforms (Columns 3, 4, 5) obtained from all recording locations provide direct evidence that brain systems compute orthogonal eigenfunctions to represent the attribute dimensions and exemplars embodied within an orthogonal stimulus set. Fig. 15.6 presents squared correlation coefficients (i.e., % predictability) printed next to each ΔEP waveform-pair to index the strength of the experimental effects. Column 3 shows that the form dimension contained nearly perfect basis waveform-pairs, with predictabilities of no less than 95%. Column 4 shows that the color dimension contained less well determined basis waveform-pairs, with an average predictability of 75%. Finally, Column 5 presents the averaged ΔEP waveform-pairs for the form and color dimensions which show that the brain orthogonalized the basis waveforms with an average error of 7.3%.

We repeated the same procedures with data sets obtained from the concept-format classification experiments (Hudspeth & Alexander, 1993). Fig. 15.8 presents the results of these calculations for 16 electrode locations. These findings are presented in the same format as those shown in the Summary of PCA results presented in Fig. 15.7B. For a direct comparison, note the electrode identified as "F4" in Fig. 15.7. It can be seen that the EP waveforms for cat and cup in Fig. 15.8 (Column 1) vary symmetrically around the exogenous EP waveshape computed for the FC cell of the stimulus matrix. Similarly, the EP waveforms for picture and word in Fig. 15.8 (Column 2) also vary symmetrically around the exogenous EP waveshape. While the EP waveforms for each stimulus are the same as those depicted in Fig. 15.7B, note that the exogenous EP waveform in Fig. 15.8: (FC average) is identical to the exogenous basis waveform (Component 1) obtained from the PCA method (Fig. 15.7B). Similarly, the ΔEP waveform-pairs for cat and cup in Fig. 15.8 (Column 3) are identical in shape and polarity to the second basis waveform (Component 2) obtained from the PCA method (Fig. 15.7B). Finally, the ΔEP waveform-pairs for picture and word in Fig. 15.8 (Column 4) are identical in shape and polarity to the third basis waveform (Component 3) obtained from the PCA method (Fig. 15.7B).

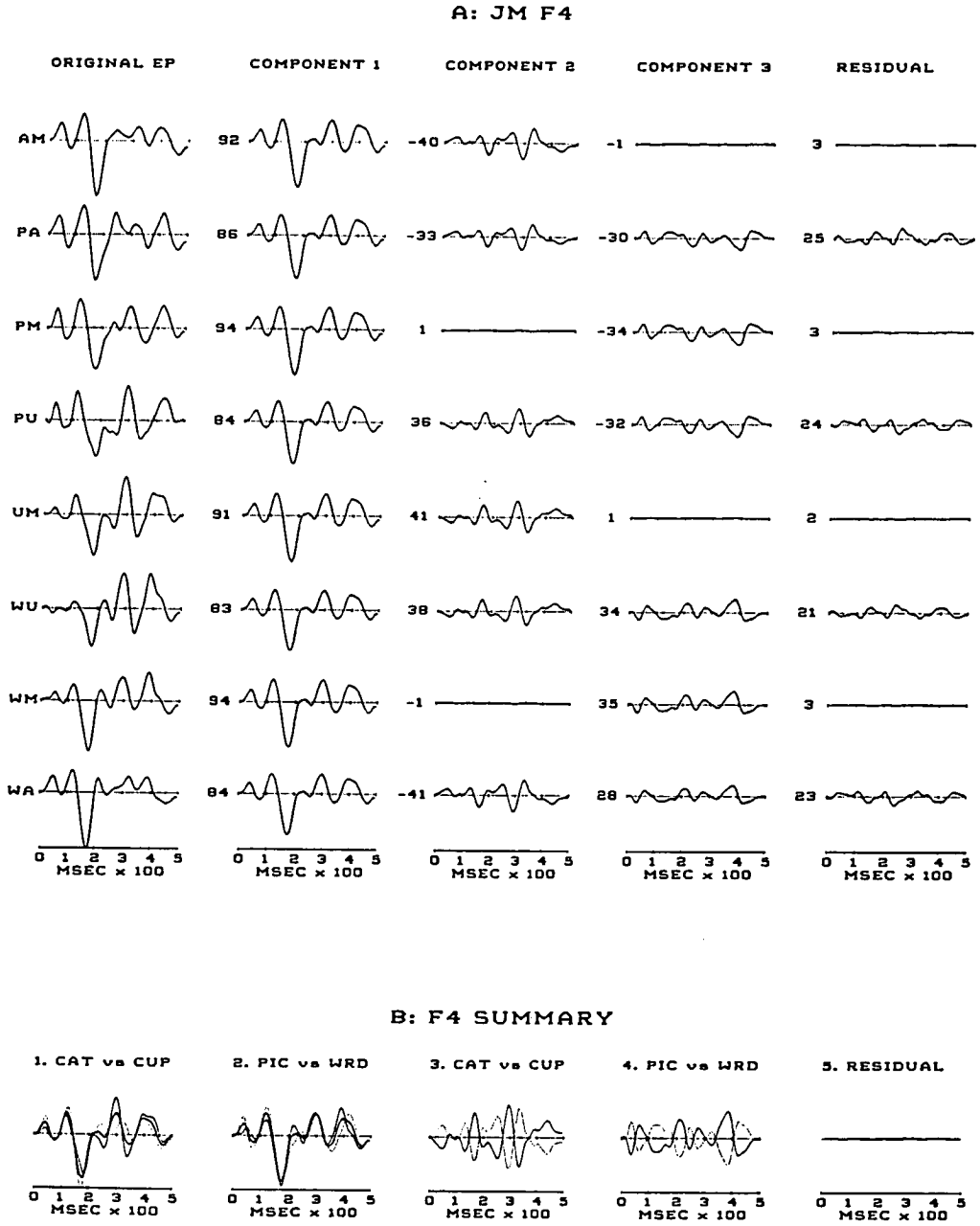

Fig. 15.7. Fig. 15.7A presents the results of a principal components analysis (PCA) for the right dorso-frontal (F4) electrode in the concept-format classification experiment. Column 1 presents the ORIGINAL EP waveforms for the 8 stimulus positions on the unit-circle model: AM — cat mean, AP — picture cat, PM — picture mean, PU — picture cup, UM — cup mean, UW — word cup, WM — word mean and AW — cat word. Column 2 presents Component 1, the exogenous basis waveform for each stimulus position. Column

Fig. 15.8 shows that the ΔEP waveform-pairs (Columns 3, 4, 5) obtained from all recording locations provide direct evidence that brain systems compute orthogonal eigenfunctions to represent the attribute dimensions and exemplars embodied within an orthogonal stimulus set. Fig. 15.8 presents squared correlation coefficients (i.e., % predictability) printed next to each ΔEP waveform-pair to index the strength and direction of the experimental effects. Column 3 shows that the concept dimension contained nearly perfect basis waveform-pairs, with predictabilities of no less than 90%. Column 4 shows that the format dimension contained slightly less well determined basis waveform-pairs, with an average predictability of 86.6%. Finally, Column 5 presents the averaged basis waveform-pairs for the concept and format dimensions which show that the brain orthogonalized the basis waveforms with an average error of 7.7%.

3.4. NEUROELECTRIC TRANSFER FUNCTIONS FOR CONCEPTUAL CLASSIFICATIONS

It will be recalled that we modeled these experiments on the methods of mathematical psychology, in which mental representation is defined as the ability of human subjects to co-relate stimulus attributes according to meaningful dimensions embedded within a set of stimuli. Further, the fact that different subjects provide the same behavioral interpretations for a configuration of stimulus attributes can be taken as evidence that the subjects share a common set of meanings which are based upon each subject's mental representations. In much the same manner, we intended to intrude into subject interpretations well before behavioral action was required, so that we could determine whether the brain's neuroelectric behaviors would provide similar interpretations for the configuration of stimulus attributes embodied in the orthogonal stimulus sets we used. Therefore, our experiments can be interpreted in the same manner as behavioral studies of mental representation, with the exception that, in our experiments, the observed interpretations arise from cortical computations. We reasoned that a conceptual transfer function could be defined by the agreement between the *a priori* predictor model (i.e., Figs. 15.3B & 15.4B) and the configuration of the 8 ΔEP basis waveforms that represent an orthogonal stimulus set, as exemplified in the form-color and concept-format experiments.

We computed transfer functions for each recording electrode, based upon the 8 deviation (ΔEP) waveforms used to represent a stimulus matrix. To avoid individual differences in ΔEP waveforms, the transfer functions were determined for each individual subject before estimating group statistics. Again, we used PCA to compute the conjoint similarities and dissimilarities among the 8 ΔEP waveforms to obtain the weighting coefficients needed to project each of the waveforms onto the circumference of a unit-circle. The results of these calculations allowed us

---

3 presents Component 2, the concept basis waveform for each stimulus position. Column 4 presents Component 3, the format basis waveform, for each stimulus position. Column 5 presents the RESIDUAL waveform which obtains after removal of the first three the basis waveforms. Weighting coefficient are presented to the left of each basis and residual waveform to index the magnitude of the specific basis waveform. The coefficients should be read as: C/100 as they were scaled for printing. A 500 millisecond time index is placed under each of the five waveform columns. Fig. 15.5B present a SUMMARY of the PCA findings for the F4 electrode that is formatted for direct comparisons with the calculations shown in Fig. 15.8. The text describes these comparisons. (From: Hudspeth, 1993a; Hudspeth & Alexander, 1993).

to make direct comparisons between the *a priori* model and the observed conceptual transfer functions.

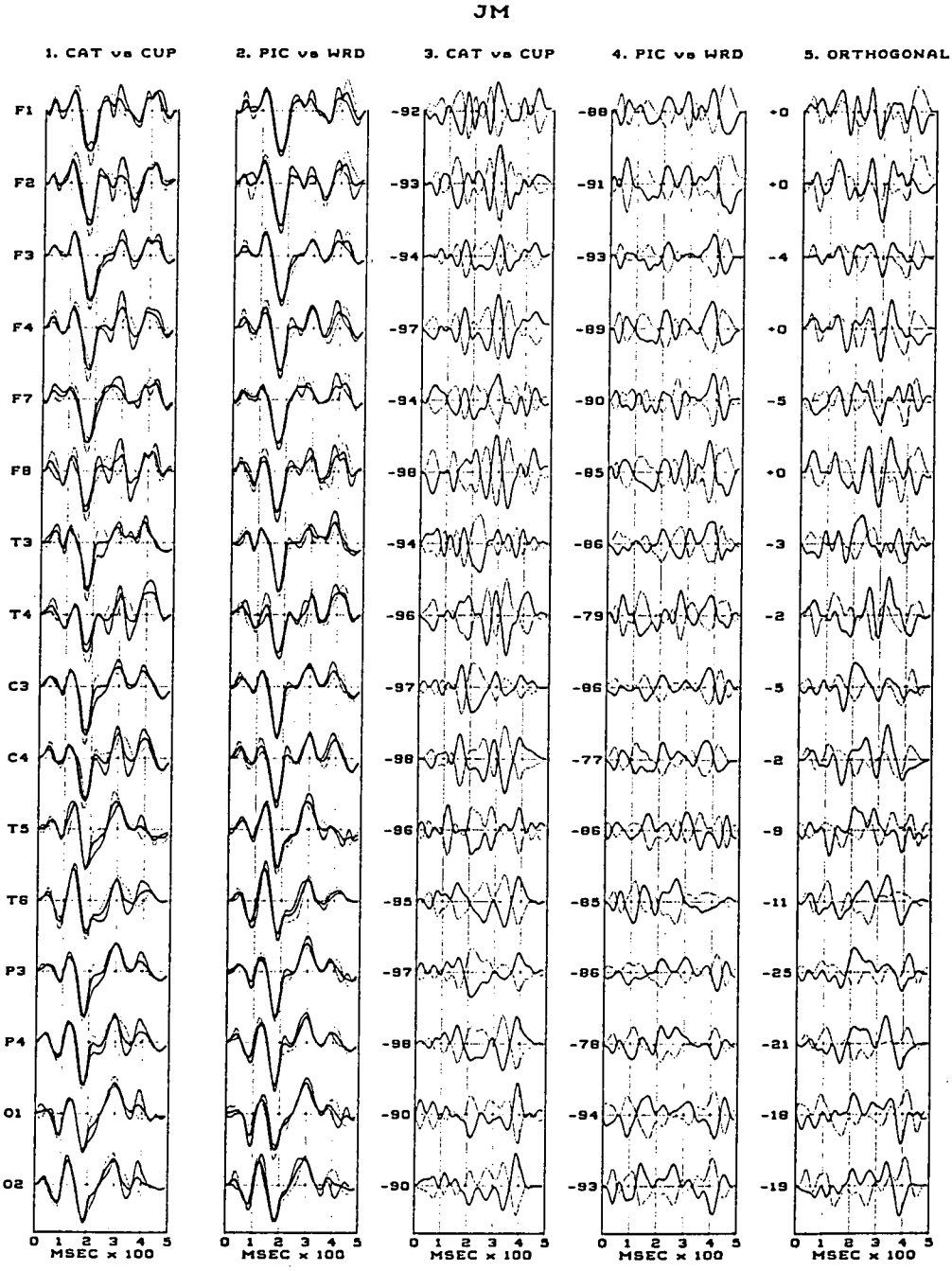

Fig. 15.8. Presents the EP and ΔEP waveforms obtained for the concept-format classification experiment. Columns 1 presents the EP waveforms for the cat and cup means. Note that, at each electrode location, these waveforms deviate symmetrically around the local exogenous EP waveform (shown as a thick line). Similarly,

Fig. 15.9A presents the averaged (N = 8 subjects) transfer functions for the eight recording electrodes used in the form-color classification studies (Hudspeth, 1993). The PCA analyses accounted for more than 83% of the covariance within all of the transfer functions. Fig. 15.9B presents scatter-plots for the observed transfer functions (Y) and the predictive model (X), measured as the angular position (degrees of arc) of each ordered pair (X, Y) on the circumference of a unit-circle. The nonparametric correlations between the predictive model and the observed transfer functions were equal to 1.0 at all electrode positions. We also computed the distribution of angular errors of the observed vectors around their expected angular positions on the unit-circle, and in general, color attributes had a weaker influence on the transfer functions than did the form attributes. These findings also provide robust support for the primary hypothesis with respect to intra-compartmental computations which are based upon EP waveforms.

Fig. 15.10 presents the averaged (N = 12 right handed subjects) transfer functions for the 16 recording electrodes used in the concept-format classification studies (Hudspeth & Alexander, 1993). The PCA analyses accounted for an average of better than 80% of the covariance within each transfer function, and the texture gradients shown in Fig. 15.10 describe the averaged regional differences in the observed cumulative eigenvalues. The nonparametric correlations between the predictive model and the observed transfer functions were equal to 1.0 at all electrode positions. These findings also provide robust support for the primary hypothesis with respect to intra-compartmental computations which are based upon EP waveforms.

4. DISCUSSION

4.1. SURVEY OF FINDINGS

This review of investigations from our laboratory has shown that spontaneous (SP) and evoked (EP) neuroelectric signals can be used to address a number of issues in cognitive neuroscience. For example, this review has shown that the age-dependent changes in SP waveforms obtained from different computational systems are highly correlated with a general

---

Columns 2 presents the EP waveforms for the picture and word means. Note that, at each electrode location, these waveforms also deviate symmetrically around the local exogenous EP waveform (shown as a thick line). When the local exogenous EP waveform was removed, ΔEP waveform-pairs for the concept axis and the format axis were nearly identical and sign-inverted. In contrast, ΔEP waveform-pairs for the orthogonal axes were effectively uncorrelated. The sign and magnitude of the squared correlation coefficients (r^2) for each pair of ΔEP waveform is presented to the left of the tracings for each recording location and axis comparison (concept, format and orthogonal). *Data Tracings:* Each waveform-pair is composed of dotted and solid line tracings that identify primary features named in each Figure heading. In all cases, the first named feature is the dotted line, and the second named feature is the solid line. *Scaling Factors*: The epoch length of each waveshape was 500 msec, using 100 points with 5 msec/point resolution. The amplitude of all EP waveforms was equated by transformation to a Z-Score scale with a Mean = 0, and σ = 1.0. Please note that the scaling for ΔEP waveforms is twice that of EP waveforms. (From: Hudspeth, 1993a; Hudspeth & Alexander, 1993).

model of cognitive maturation. Further, this review has shown that the functional integration of different computational systems can be reliably predicted from the organization of neuroanatomical systems by means of 3-basis waveform vectors extracted from multichannel SP waveforms. Finally, this review has shown that EP waveforms provide transfer functions for perceptual and conceptual classifications by means of orthogonal basis waveforms which arise within different computational systems.

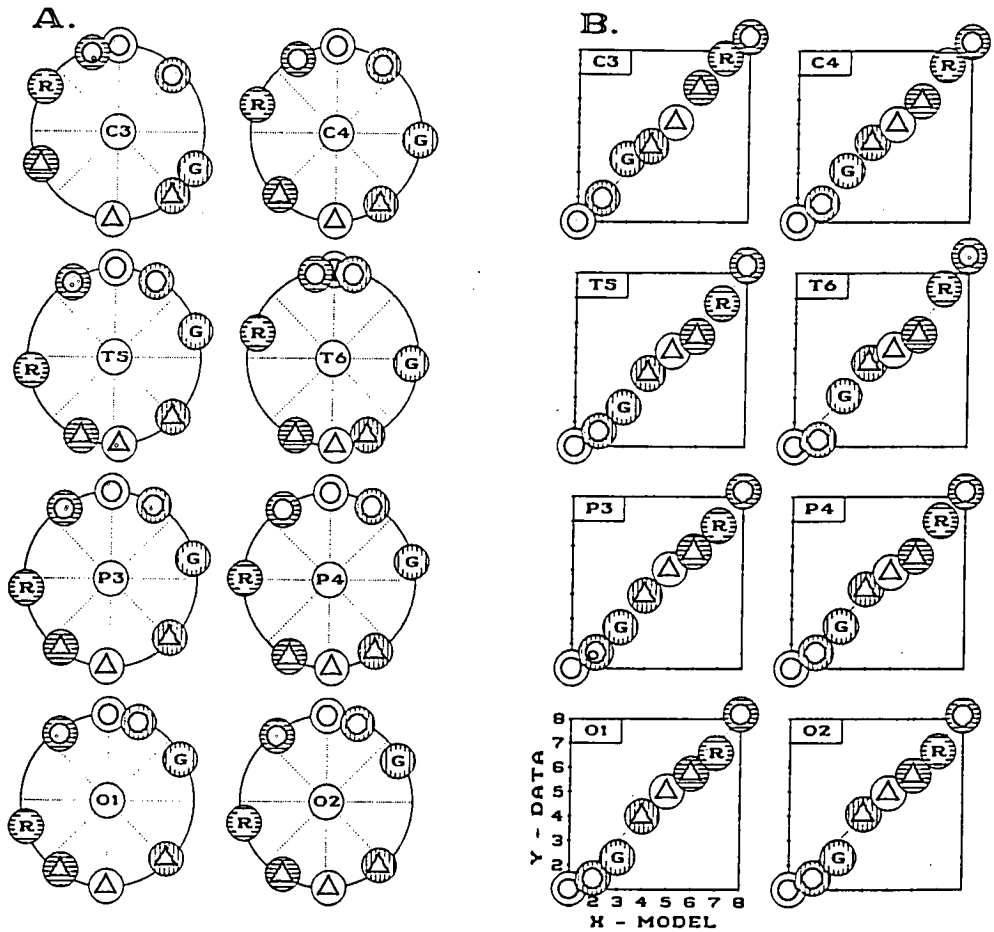

Fig. 15.9. Presents a graphic analysis of the form-color transfer functions for each electrode location. Fig. 15.8A presents the observed output transfer functions for each electrode location. These results show how well the observed ΔEP data sets reproduce the unit-circle classification. Fig. 15.8B presents scattergrams based upon the *a priori* model (MODEL - X axis) and the averaged transfer functions (DATA = Y axis). *Symbol Key:* circle, triangle, green and red features are represented by the same graphic coding scheme as shown in Fig. 15.3. (From Hudspeth, 1993b).

Taken as a whole, the findings reported here imply that, in a well designed investigation, using a representative set of SP and EP measures, it would be possible to examine a subject's specific cognitive abilities (EP classifications), determine the origin and integration of the computational systems that generate these signals (SP structures), and as well, provide an estimate of the subject's level of cognitive maturation. While we are some distance from this goal, most of the work in my laboratory is directed toward this outcome. What seems most important, is that this approach seems to result in a high level of theoretical and empirical integration as it pertains to the study of neuroelectric signals and functional neuroscience.

4.2. IN SEARCH OF A PROCESS

Of particular interest here are the investigations which were designed to explore the primary hypothesis concerning the generation of neuroelectric basis waveforms that: a.) reveal the global integration of computational systems and b.) provide transfer functions for mental representations within computational systems. Our findings show that the integration of computational systems (SP waveforms) are determined by 3 basis waveforms which account for approximately 85% of the covariation within a multichannel SP recording. While we have intensified our search for additional basis waveforms (or noise), it is nonetheless true that the complexities of a multichannel SP recording are completely (i.e., 85%) reducible to 3-dimensions which have exquisite neuroanatomical accuracy in the horizontal, sagittal and coronal planes, respectively. Therefore, it is reasonable to entertain the hypothesis that the functional systems of the brain comprise a closed (i.e., finite-dimensioned) Hilbert space, which is based upon a finite number of interconnected neuronal generator systems.

Moreover, it is also the case that each neuronal generator system provides, in EP waveforms, the exact number of signed basis waveforms (i.e., is completely reducible) needed to account for the dimensions and exemplars embodied in perceptual and conceptual classifications. Again, I am inclined toward the same hypothesis: first, that mental representations are constructed by means of waveform eigenstructures within a unitary Hilbert space (i.e., neuroanatomical system), and second, that these observed behaviors suggest that major brain systems are *computational* compartments. (For a discussion of Hilbert spaces, see: Hamermesh, 1989; pp. 68-114).

For those who are more comfortable with intracerebral recordings from single and multiple neuron(s), Young and Yamane (1992) have recently shown that macaque anterior inferotemporal cells are able to classify human faces (i.e., photographs) by means of two attribute dimensions that coexist (i.e., a linear combination) in cell discharge patterns, and which are sufficient to uniquely identify 27 different faces. If we concur with traditional mechanisms for generating action potentials, then the underlying slower dendritic potentials may likely behave according to the principles of a Hilbert space.

4.3. IN SEARCH OF A MECHANISM: SAND, LIGHT AND NEURON

It is not entirely satisfying to propose a fairly accurate process by means of which computational systems could accomplish mental representations without some discussion (even speculation) of the neurohistological fabric that might mediate such computations. This

discussion is also relevant for efforts to construct realistic neural networks; i.e., able to perform conceptual transformations.

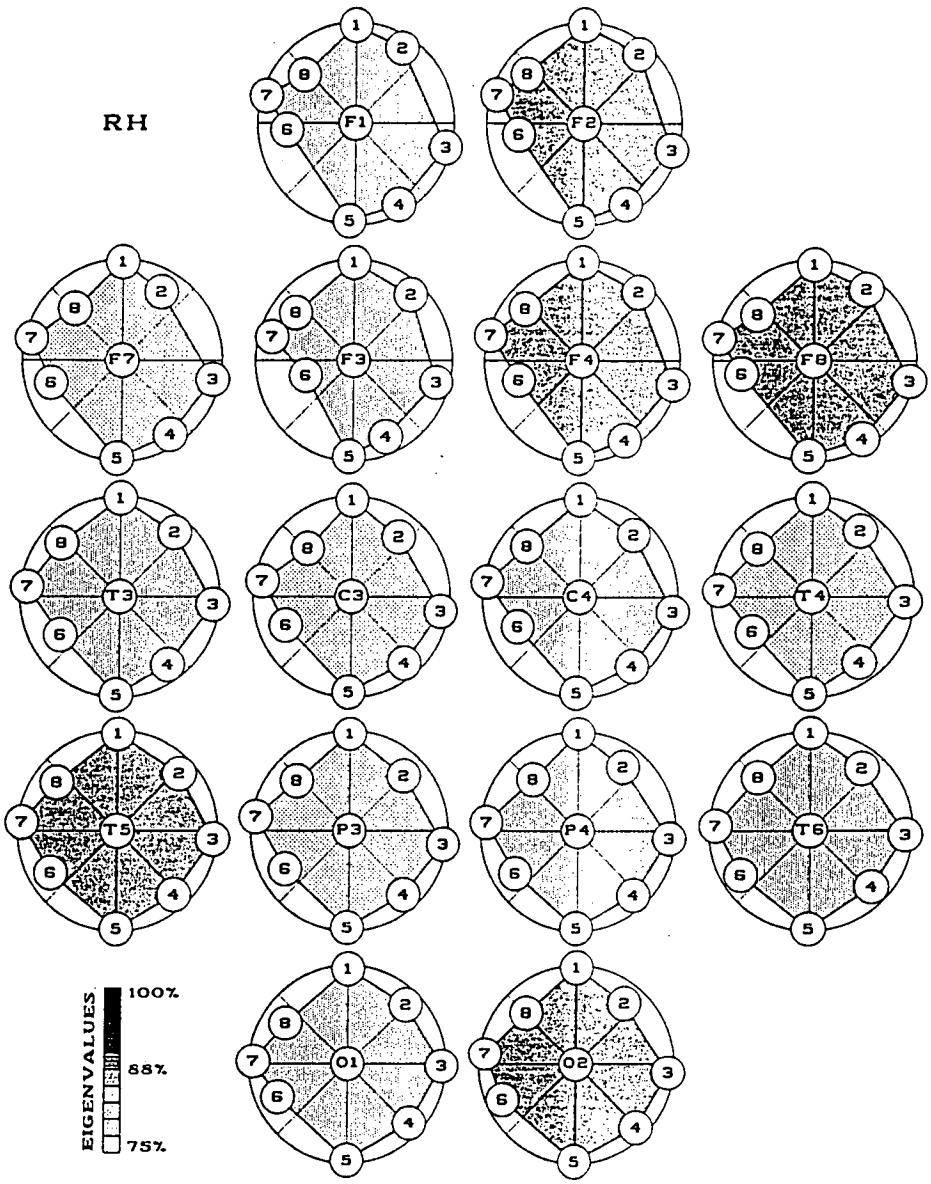

Fig. 15.10. Presents a graphic analysis of the concept-format transfer functions for each electrode location, based upon averages from 12 right handed subjects. The cumulative eigenvalues for each electrode is scale between 75%-100%, and the texture plotted within each of the 16 drawings provides an index for each electrode. *Symbol Key:* cat, cup, picture and word features are represented by the same graphic coding scheme as shown in Fig. 15.4.

Slightly more than fifty years after the psychological sciences were founded, several workers began to recognize fundamental flaws in theories of how the brain represents direct experience and memories of direct experience. Those concerns centered on both the processes and structures needed to accomplish such representations. On one hand, specific experiences and their memories might reside in specific cortical regions. But then, were the storage locations infinite or finite? That could be a problem. On the other hand, specific experiences and their memories could be etched into selective synaptic pathways known as traces. But then, could new traces overwrite older traces? That could be a problem too. With these problems in mind, some workers proposed dynamic (i.e., re-writable) traces (Köhler, 1923). Unfortunately, dynamic traces still posed a serious threat to older traces.

Wheeler and Perkins (1932) were the first workers to implement *interference patterns*, a dynamic non-trace model, for mental representation and memory reconstruction. Further, they assumed that cognitive complexity was based upon brain maturation and differentiation, such that the representational skill of brain systems naturally expanded to encompass new experiences and memories. They employed a mechanical analogy, called Chladni's plate, upon the surface of which a layer of vibrating sand could be made to partition itself according to perturbations with additional vibratory stimuli.

Eighteen years later, Lashley (1950) reported on his 30 year series of experiments in which he removed varying amounts, in varying locations, of the rodent cerebrum, so that he could localize and characterize memory processes. He was conclusive about the fact that, as he removed larger areas of the cortex, memory deficits increased. However, he was unable to find any particular cortical region that was required in memory processes. He concluded that experience and memory might be based upon neuroelectric interference patterns that were widely distributed across the cerebrum, such that memories could be retained in the presence of large cortical lesions. It should be clear that the lissencephalic structure of the rodent cerebrum is not a proper model for the structures and functions of the human brain, and that Lashley's principles may not apply. However, I would want to retain his conclusions regarding neuroelectric interference patterns.

It was not until Gabor's (1946) discovery of the optical hologram that a number of workers recognized a very realistic and life-like instantiation of the interference pattern (Westlake, 1967; Willshaw, Buneman, & Longuet-Higgins, 1969; Van Heerden, 1970; Pribram, 1971, 1991; Hudspeth & Jones, 1975, 1977). The holographic model was appealing because images and memories of images could be distributed across the entire surface of a representational system, and a complete image, albeit of low resolution, could be reconstructed from a small fragment of the representational system and, thus, could sustain the types of lesions Lashley applied to the rodent brain. However, there are substantial difficulties in the neural holographic model. First, an optical hologram *requires* both a linear reconstruction surface and, as well, linear reference and object signals. Neither of these conditions obtain within the computational systems of the brain. Moreover, there are perceptual demonstrations which clearly obviate the existence of neural holograms. First, nearly all introductory psychology textbooks provide a demonstration for locating the eyes' blind-spots, the retinal location from which the optic nerve leaves the eye, and at which, there are no photic receptors. By using monocular vision, the blind-spot can be located at about 7° beyond the point of fixation in the temporal visual field, and nothing can be seen within the region of this very small hole. Similarly, individuals with

punctate lesions of the primary striate cortex have a deficit called central blindness, in which the portion of the visual field which is mapped by the injured cortex is experienced as an empty hole. Neither of these exceptions should occur if neural holograms provided the means for mental representation.

While the brain's computational systems are not linear, these surfaces can provide undistorted transformations of sensory input (i.e. images) by means of the neurohistological geometries of cortical mapping surfaces. For example, Schwartz (1980) has provided a detailed description for the geometry of the primary visual cortex. The significant components of this geometry are composed of the striate boundaries and the spatial density of vertical columns and hypercolumns confined within those boundaries. Schwartz characterized the boundaries of the striate system in several mammalian species, and according to his calculations the striate system can, in general, be considered a *simply connected domain*, in which retinal information is preserved by means of conformal transformation. Conformal transformation is significant for cognitive neuroscience because it is a means by which perceptual constancies (invariance with dilation, rotation & translation) can be preserved within a computational domain.

Further, Schwartz estimated the spatial distribution of receptive fields within the striate system. This distribution could be described by a range of receptive field sizes and proximities which are small and dense in the striate representation of the fovea and which increased logarithmically in the striate representation of eccentricity in the peripheral field. This logarithmic function constitutes a gradient of magnification which plays an important role in forming a unitary computational space in which the eigenfunctions of mental representation can obtain. The adjacency of vertically oriented columns and hypercolumns within the striate system provides the means for interactions among the dendritic potentials arising from constituent columnar structures. However, the term "interaction" is far too vague for my intent or comfort. I would rather specify that these interactions are composed of the conjoint similarities-dissimilarities in the dendritic potentials arising from constituent columnar structures. My formulation implies that computational systems have internal correlation and eigenfunction processors, a notion for which there is no immediate evidence.

There may be a more satisfactory and simple solution to this problem. It is well know that columnar structures have unique tuning characteristics (eye, color, spatial frequency, orientation), and it might be expected that their dendritic potentials would reflect this selective characteristic. Dendritic potentials in adjacent columns can be expected to have a partial coherence which is preserved in the algebraic sum of the two potentials. It can be seen that the algebraic sum of similar potentials will preserve the coherent feature, and conversely, the algebraic sum of dissimilar potentials fails to provide a coherent feature. Thus, at any moment in time, the striate mapping system is primarily composed of coherent dendritic potentials that reflect only a selected set of tuning features. However, when a subject's fovea is fixed on a stimulus, the cortical magnification factor (i.e., logarithmic gradient) provides an amplification of coherent dendritic potentials which is proportional to the eccentric position in the visual field. In the region of foveal representation, all of the coherent dendritic potentials are effectively multiplied by means of the algebraic sum of numerous and densely packed receptive fields. This magnification is achieved in much the same manner as the summation of a Fibonacci series, except that here, the distance between elements (i.e., receptive fields) is logarithmic. The complete global mapping of the striate system should now contain a field of magnified coherent

dendritic potentials that are based upon a selected set of receptive fields which are driven by the stimulus attributes viewed by the subject. There are two generalizations that follow from this analysis. The first deals with the interpretation of the coherent waveforms and the second deals with the visual image embedded within the mapping function.

If coherent dendritic potentials reflect only the common attribute sources in the visual field, then I am tempted to suggest that these potentials are the basis waveforms from which perceptual and conceptual representations are constructed. In effect, this mapping represents the common cross-products of uniquely tuned features, which is simply a different way to say that the striate system constructed eigenfunctions by means of selective summation and amplification of coherent dendritic waveforms. The EP studies reported in this chapter suggest that this notion could be sound.

Finally, Schwartz (1980) suggests that the visual image is enfolded within the forward Radon transformation of the conformal mapping function, and that the image could be instantiated (i.e., extracted) with an inverse Radon transformation. It is reasonable to believe that these analytic methods could provide valuable information about image formation in the striate system. However, as with other efforts to endow cortical tissues with sophisticated analytic prowess (FFTs, hologram), there is the potential for falling into analytic solipsism. Could these principles be demonstrated in convergent measurements or procedures? Preferably, such measurements need to be made in such a way as to: a.) bridge the distinctions between cells and systems; and b.) apply to the most complex perceptual or conceptual task possible.

REFERENCES

Begleiter, H., & Porjesz, B. (1975). Evoked brain potentials as indicators of decision making. *Science* **187**, 754-755.

Begleiter, H., Porjesz, B., & Garozzo, R. (1979). Visual evoked potentials and affective ratings of semantic stimuli. In H. Begleiter (Ed.), *Evoked Brain Potentials and Behavior*. New York: Plenum Press.

Boddy, J. (1985). Brain event-related potentials in the investigation of language processing. In: D. Papakostopoulos, S. Buttler, & I. Martin (Eds.), *Clinical and Experimental Neuropsychophysiology*. London: Croom Helm.

Buchsbaum, M., Coppola, R., & Bittker, T. E. (1974). Differential effects of congruence, stimulus meaning and information on early and late components of the averaged evoked response. *Neuropsychologia* **12**, 533-545.

Case, R. (1992). Role of the frontal lobes in the regulation of cognitive development. *Brain and Cognition* **20**, 51-73.

Gabor, D. (1946). Theory of communication. *Journal of the Institute of Electrical Engineers* **93**, 429-441.

Hamermesh, M. (1989). *Group Theory and It's Applications to Physical Problems*. New York: Dover.

Hillyard, S. A., Picton, T. W., & Regan, D. (1978). Sensation, perception and attention: Analysis using ERPs. In E. Callaway, P. Tueting, & S. H. Koslow (Eds.), *Event-related Brain Potentials in Man*. New York: Academic Press.

Hillyard, S. A., & Picton, T. W. (1979). Event-related brain potentials and selective information processing in man. In J. E. Desmedt (Ed.), *Progress in Clinical Neurophysiology, Vol. 6, Cognitive Components in Cerebral Event-related Potentials and selective Attention,* J. E. Desmedt (Ed.) Basel: Karger.

Hudspeth, W. J. (1985). Developmental neuropsychology: Functional implications of quantitative EEG maturation [Abs]. *Journal of Clinical and Experimental Neuropsychology* 7, 606.

Hudspeth, W. J. (1987). Symposium on functional neuroscience: Neurophysiological correlates of Piagetian maturation. Meeting of Western Psychological Association, Long Beach, CA.

Hudspeth, W. J. (1990, July). VEPs and dimensions of visual perception. *Proceedings of the Fifth International Congress of Psychophysiology, [abs],* 132.

Hudspeth, W. J. (1993a). Neurocybernetic devices. U. S. Patent and Trademark Office,Washington, DC: Pending.

Hudspeth, W. J. (1993b). Neuroelectric concepts: Form-color classification. *Brain and Cognition* 21, 226-246.

Hudspeth, W. J., & Alexander, J. E. (1993). Neuroelectric concepts: Word-picture classification. Submitted for publication.

Hudspeth, W. J., Alexander, J. E., & Garrett, A. S. (1993). Functional architecture of the human electroencephalogram. Unpublished manuscript.

Hudspeth, W. J., & Jones, G. B. (1975). Stability of neural interference patterns. *Holography in Medicine.* Guilford, England: I.P.C. Science and Technology Press.

Hudspeth, W. J., & Jones, G. B. (1977). Neural models for short-term memory. *Neuropsychologia* 16, 201-212.

Hudspeth, W. J., & Pribram, K. H. (1990). Stages of brain and cognitive maturation. *Journal of Educational Psychology* 82, 880-883.

Hudspeth, W. J. & Pribram, K. H. (1992). Psychophysiological indices of cerebral maturation. *International Journal of Psychophysiology* 12, 19-29.

John, E. R., Harrington, R. N., & Sutton, S. (1967). Effects of visual form on the evoked response. *Science* 155, 1439-1442.

John, E. R. (1977). *Functional Neuroscience (Vol.2): Neurometrics: Clinical Applications of Quantitative Neurophysiology.* Hillsdale, NJ: Lawrence Erlbaum Associates.

John, E. R., & Schwartz, E. L. (1978). The neurophysiology of information processing and cognition. *Annual Review of Psychology* 29, 1-29.

Johnston, V. L., & Chesney, G. L. (1974). Electrophysiological correlates of meaning. *Science* 186, 944-946.

Kohler, W. (1923). Zur theorie des Sukzessivvergleichs und der Zeitfehler. *Psychologie Forschungen* 4, 115-175.

Lashley, K. S. (1950). In search of the engram. *Symposium of the Society of Experimental Biology.* Cambridge, England: Cambridge University Press.

Luria, A. R. (1973). *The Working Brain: Introduction to Neuropsychology.* New York: Basic Books.

Luria, A. R. (1980). *Higher Cortical Functions in Man.* New York: Basic Books.

Wheeler, R. H., & Perkins, F. T. (1932). *Principles of Mental Development.* New York: T. Y. Crowell.

Young, M. P., & Yamane, S. (1992). Sparse population coding of faces in the inferotemporal cortex. *Science 256*, 1327-1331.

Piaget, J. (1963). *The Origins of Intelligence in Children.* New York: W. W. Norton & Company.

Pribram, K. H. (1971). *Languages of the Brain: Experimental Paradoxes and Principles in Neuropsychology.* Englewood Cliffs, NJ: Prentice-Hall.

Pribram, K. H. (1991). *Brain and Perception: Holonomy and Structure in Figural Processing.* Hillsdale, NJ: Lawrence Erlbaum Associates.

Regan, D. (1972). *Evoked Potentials in Psychology, Sensory Physiology and Clinical Medicine.* New York: Wiley-Interscience.

Roemer, R. A., & Teyler, T. J. (1977). Auditory evoked potential asymmetries related to word meaning. In J. Desmedt (Ed.), *Progress in Clinical Neurophysiology, Vol. 3. Language and Hemispheric Specialization in Man: Cerebral Event-Related Potentials.* Basel: Karger.

Schwartz, E. L. (1980). Computational anatomy and functional architecture of striate cortex: A spatial mapping approach to perceptual coding. *Vision Research* **20**, 645-669.

Shelburne, S. A., Jr. (1973). Visual evoked response to language stimuli in children With reading disabilities. *Electroencephalography and Clinical Neurophysiology, 34*: 135-143.

Shepard, R. N. & Chipman, S. (1970). Second-order isomorphism of internal representations: Shapes of states. *Cognitive Psychology* **1**, 1-17.

Shepard, R. N. (1975). Form, formation and transformation of internal representations. In: R. Solso (Ed.), *Information Processing and Cognition: The Loyola Symposium.* Hillsdale, NJ: Lawrence Erlbaum Associates.

Shepard, R. N. (1978). The mental image. *American Psychologist* **33**, 125-137.

Shepard, R. N., Kilpatric, D. W., & Cunningham, J. P. (1975). The internal representation of numbers. *Cognitive Psychology* **7**, 82-138.

Stuss, D. T. (1992). Biological and psychological development of executive functions. *Brain and Cognition* **20**, 8-23.

Teyler, T. J., Roemer, R. A., Harrison, T. F., & Thompson, R. F. (1973). Human scalp-recorded evoked-potential correlates of linguistic stimuli. *Bulletin of the Psychonomic Society* **1**, 333-334.

Thatcher, R. W., Walker, R. A., & Guidice, S. (1987). Human cerebral hemispheres develop at different rates and ages. *Science* **236**, 1110-1113.

Thatcher, R. W. (1991). Are rhythms of human cerebral development traveling waves? *Behavioral and Brain Sciences* **14**, 575.

Vandermaas, H. L. J., & Molenaar, P. C. M. (1992). Stage-wise cognitive development: An application of catastrophe theory. *Psychological Review* **99**, 395-417.

van Geert, P. (1991). A dynamic systems model of cognitive and language growth. *Psychological Review* **98**, 3-53.

Van Heerden, P. J. (1970). Models of the brain. *Nature* **225**, 177-178.

Westlake, P. R. (1967). Towards a theory of brain functioning: The possibilities of a neural holographic process. *20th Annual Conference on Engineering in Medicine and Biology,* Boston.

Willshaw, D. J., Buneman, O. P., & Longuet-Higgins, H. O. (1969). Nonholographic associative memory. *Nature* **222**, 960-962.